Biogeosciences Discuss., doi:10.5194/bg-2015-621, 2016
Manuscript under review for journal Biogeosciences
Published: 18 January 2016

Ecological Controls on N_2O Emission in Surface Litter and Near-surface Soil of a Managed Pasture: Modelling and Measurements

Grant, R.F.[1], Neftel, A.[2] and Calanca, P.[2]

[1] *Department of Renewable Resources, University of Alberta, Edmonton, AB, Canada T6G 2E3*

[2] *Agroscope Institute for Sustainability Sciences ISS, Reckenholzstrasse 191 , P.O. Box CH – 8046 Zürich, Switzerland*

ABSTRACT

Large variability in N_2O emissions from managed grasslands may occur because most emissions originate in surface litter or near-surface soil where variability in soil water content (θ) and temperature (T_s) is greatest. To determine whether temporal variability in θ and T_s of surface litter and near-surface soil could explain that in N_2O emissions, a simulation experiment was conducted with *ecosys*, a comprehensive mathematical model of terrestrial ecosystems in which processes governing N_2O emissions were represented at high temporal and spatial resolution. Model performance was verified by comparing N_2O emissions, CO_2 and energy exchange, and θ and T_s modelled by *ecosys* with those measured by automated chambers, eddy covariance (EC) and soil sensors at an hourly time-scale during several emission events from 2004 to 2009 in an intensively managed pasture at Oensingen, Switzerland. Both modelled and measured events were induced by precipitation following harvesting and subsequent fertilizing or manuring. These events were brief (2 – 5 days) with maximum N_2O effluxes that varied from < 1 mg N m^{-2} h^{-1} in early spring and autumn to > 3 mg N m^{-2} h^{-1} in summer. Only very small emissions were modelled or measured outside these events. In the model, emissions were generated almost entirely in surface litter or near-surface (0 – 2 cm) soil, at rates driven by N availability with fertilization vs. N uptake with grassland regrowth, and by O_2 limitation from wetting relative to O_2 demand from respiration. In the model, NO_x availability relative to O_2 limitation governed both the reduction of more oxidized electron acceptors to N_2O and the reduction of N_2O to N_2, so that the magnitude of N_2O emissions was not simply related to surface and near-surface θ and T_s. Modelled

Biogeosciences Discuss., doi:10.5194/bg-2015-621, 2016
Manuscript under review for journal Biogeosciences
Published: 18 January 2016

N_2O emissions were found to be sensitive to defoliation intensity and timing (relative to that of fertilization) which controlled plant N uptake and soil θ and T_s prior to and during emission events. In a model sensitivity study, reducing LAI remaining after defoliation to one-half that under current practice and delaying harvesting by 5 days raised N_2O emissions by as much as 80% during subsequent events and by an average of 43% annually. The global warming potential from annual N_2O emissions in this intensively managed grassland largely offset those from net C uptake in both modelled and field experiments. However model results indicated that this offset could be adversely affected by suboptimal harvest intensity and timing.

INTRODUCTION

The contribution of managed grasslands to reducing atmospheric greenhouse gas (GHG) concentrations through net uptake of CO_2 (Ammann et al., 2005) may be at least partially offset by net emissions of N_2O (Conant et al., 2005, Fléchard et al., 2005). These emissions may be substantial, with N_2O emission factors of as large as 3% measured in intensively managed grasslands with fertilizer rates of 25 - 30 g N m^{-2} y^{-1} (Imer et al., 2013; Rafique et al., 2011) These emissions are highly variable temporally and spatially because they are determined by complex interactions among short-term weather events (warming, precipitation) and land management practices (N amendments, defoliation). The N_2O driving these emissions in managed grasslands is thought to be generated within the upper 2 cm of the soil profile (van der Weerden et al., 2013) and in surface litter left by grazing or harvesting (Pal et al., 2013) so that diurnal heating and precipitation events that cause rapid warming and wetting of the litter and soil surface may cause large but brief emission events. These events are thought to be driven by increased demand for electron acceptors by nitrification and denitrification, and reduced supply of O_2 by which these demands are preferentially met, and therefore increased demand for alternative acceptors NO_3^-, NO_2^- and N_2O by autotrophic and heterotrophic denitrifiers.

The magnitude of N_2O emission events in managed grasslands generally increases with the amount of N added as urine, manure or fertilizer, and with the intensity of defoliation by grazing or cutting (Ruzjerez et al. 1994). Thus Imer et al. (2013) found a negative correlation between LAI and N_2O emissions at intensively managed grasslands in Switzerland. The increase in emissions with defoliation has been attributed to increased urine and manure deposition and soil compaction if

Biogeosciences Discuss., doi:10.5194/bg-2015-621, 2016
Manuscript under review for journal Biogeosciences
Published: 18 January 2016

defoliation is by grazing, and to reduced uptake of N and water by slower-growing plants after defoliation (Jackson et al., 2015). Both N additions and defoliation are thought to raise these emissions by increasing the supply of NH_4^+ and NO_3^-, thereby also increasing the demand for alternative e^- acceptors by autotrophic and heterotrophic denitrifiers if the supply of O_2, the preferred e- acceptor, fails to meet demand when soil water content (θ) rises with precipitation. Consequently land use practices must be considered when estimating N_2O emissions from managed grasslands.

Recognition of the effects of precipitation events and N additions on N_2O emissions has led to empirical models in which annual emission inventories are calculated directly from annual precipitation and N inputs (Lu et al., 2006), or monthly emission events are calculated from monthly precipitation, air temperature T_a, and θ (Fléchard et al., 2007). However the soil depth at which most emitted N_2O is generated (0 – 2 cm) is much shallower than that at which θ used in these models is measured (5 – 10 cm) (Fléchard et al., 2007), and the soil temperature T_s at this depth may differ from T_a. This is particularly so for grasslands in which N additions are necessarily left on the soil surface without incorporation. Thus large N_2O emissions may be caused by surface wetting from precipitation on dry soils following fertilizer application, so that deeper θ is sometimes found to be of little explanatory value in empirical models (Fléchard et al., 2007). Furthermore the response of denitrification to θ has been found in experimental studies to rise sharply with T_s, likely through the combined effects of T_s on increasing demand and reducing supply of O_2 at microbial microsites (Craswell, 1978). However the interaction between T_s and θ on N_2O emissions has not been accounted for in empirical models, although it is clearly apparent in the meta-analysis by Fléchard et al. (2007) of N_2O emissions from European grasslands.

Process models used to simulate N_2O emissions from managed grasslands must therefore explicitly represent the effects of short-term weather events on near-surface T_s and θ, as well as the effects of N additions and defoliation on near-surface NH_4^+ and NO_3^-. These models must also explicitly represent the effects of mineral N, T_s and θ on the demand for vs. supply of O_2 and alternative e^- acceptors NO_3^-, NO_2^- and N_2O, and the oxidation-reduction reactions by which these e^- acceptors are reduced. However earlier process models have usually simulated N_2O emissions as T_s -dependent functions of nitrification and denitrification rates, modified by texture-dependent functions of water-filled pore space (WFPS) (e.g. Li et al., 2005). In some models additional empirical functions of T_s

Biogeosciences Discuss., doi:10.5194/bg-2015-621, 2016
Manuscript under review for journal Biogeosciences
Published: 18 January 2016

(Chatskikh et al., 2005), or of T_s and WFPS (Schmid et al., 2001), are used to calculate the fraction of nitrification that generates N_2O, and the fraction of heterotrophic respiration R_h that drives denitrification (Schmid et al., 2001), thereby avoiding the explicit simulation of O_2 and its control on N_2O emissions. A more detailed summary of functions of mineral N, T_s and WFPS currently used to model N_2O emissions is given in Fang et al. (2015). These functions have many model-dependent parameters and function independently of each other, so that key interactions among reduced C and N substrates, T_s and θ on N_2O production may not be simulated. In none of these approaches are the oxidation-reduction reactions by which N_2O is generated or consumed explicitly represented. Futhermore the effects of defoliation and surface litter on N_2O emissions have not been considered in earlier process models.

Process models used to simulate N_2O emissions must also accurately represent the key processes of C cycling which drive those of N cycling from which N_2O is generated and consumed. These include gross and net primary productivity (GPP and NPP) which drive mineral N uptake and assimilation with plant growth. GPP and consequent plant growth also drive autotrophic respiration (R_a), the below-ground component of which contributes to soil O_2 demand. NPP drives litterfall and root exudation, which in turn drive heterotrophic respiration (R_h) that also contributes to litter and soil O_2 demand, and thereby to demand for alternative e^- acceptors which drive N_2O generation. Heterotrophic respiration also drives key N transformations such as mineralization/immobilization, thereby controlling availability of these alternative e^- acceptors. Land use practices such as defoliation from grazing or harvesting alter these key C cycling processes, and thereby N_2O emissions.

In the mathematical model *ecosys*, the effects of weather and N amendments on T_s, θ, and mineral N, and hence on the demand for vs. supply of O_2, NO_3^-, NO_2^- and N_2O, and thereby on N_2O emissions, are simulated by explicitly coupling the transport processes with the oxidation – reduction reactions by which these e^- acceptors known to be generated, transported and consumed in soils (Grant and Pattey, 1999, 2003, 2008; Grant et al., 2006; Metivier et al., 2009). In an extension of earlier work with this model, we propose that temporal variation in N_2O emissions from an intensively managed grassland can be largely explained from the modelled effects of N amendments (fertilizer, manure), plant management (harvest intensity and timing) and weather (T_s, precipitation events) on the demand for vs. supply of O_2, NO_3^-, NO_2^- and N_2O in surface litter and near-surface soil (0 – 2 cm).

Biogeosciences Discuss., doi:10.5194/bg-2015-621, 2016
Manuscript under review for journal Biogeosciences
Published: 18 January 2016

Testing this explanation requires frequent measurements to characterize the large temporal variation in N_2O emissions found in managed ecosystems. Such measurements were recorded from 2004 to 2009 using automated chambers in an intensively managed grass-clover grassland at Oensingen, Switzerland, and used here to test our modelled explanation of these fluxes.

MODEL DEVELOPMENT

General Overview

The hypotheses for N_2O transformations in *ecosys* are described below with reference to equations and definitions listed in Appendices A, C, D, E, H of the Supplement (indicated by square brackets in the text below, e.g. [H1] refers to Eq. 1 in Appendix H), as well as in earlier papers (Grant and Pattey, 1999, 2003, 2008; Grant et al., 2006; Metivier et al., 2009). These hypotheses are part of a model of soil C, N and P transformations (Grant et al., 1993a,b), coupled to one of soil water, heat and solute transport in surface litter and soil layers, which are in turn components of the comprehensive ecosystem model *ecosys* (Grant, 2001). The model is designed to be parameterized as much as possible from basic disciplinary studies conducted independently of the model.

Mineralization and Immobilization of Ammonium by All Microbial Populations

Heterotrophic microbial populations *m* (obligately aerobic bacteria, obligately aerobic fungi, facultatively anaerobic denitrifiers, anaerobic fermenters, acetotrophic methanogens, and obligately aerobic and anaerobic non-symbiotic diazotrophs) are associated with each organic substrate *i* (*i* = animal manure, coarse woody plant residue, fine non-woody plant residue, particulate organic matter, or humus). Autotrophic microbial populations *n* (aerobic NH_4^+ and NO_2^- oxidizers, hydrogenotrophic methanogens and methanotrophs) are associated with inorganic substrates. These populations grow with energy generated from coupled oxidation of reduced dissolved C (DOC) by heterotrophs, or of mineral N (NH_4^+ and NO_2^-) by nitrifiers, and reduction of e- acceptors O_2 and NO_x. These populations decay according to first-order rate constants. During growth, each functional component *j* (*j* = nonstructural, labile, resistant) of these populations seeks to maintain a set C:N ratio by mineralizing NH_4^+ ([H1a]) from, or by immobilizing NH_4^+ ([H1b]) or NO_3^- ([H1c]) to, microbial organic N. Nitrogen limitations during growth may cause C:N ratios to rise above set values, as well as greater recovery of microbial N

Biogeosciences Discuss., doi:10.5194/bg-2015-621, 2016
Manuscript under review for journal Biogeosciences
Published: 18 January 2016

from structural to nonstructural components to reduce N loss during decay, but at a cost to microbial function. These transformations control the exchange of N between organic and inorganic states, and hence affect the availability of alternative e^- acceptors for nitrification and denitrification.

Oxidation of DOC and Reduction of Oxygen by Heterotrophs

Constraints on heterotrophic oxidation of DOC imposed by O_2 uptake are solved in four steps:

1) DOC oxidation under non-limiting O_2 is calculated from active biomass, DOC concentration, and an Arrhenius function of T_s [H2],
2) O_2 reduction to H_2O under non-limiting O_2 (O_2 demand) is calculated from 1) using a set respiratory quotient [H3],
3) O_2 reduction to H_2O under ambient O_2 is calculated from radial O_2 diffusion through water films of thickness determined by soil water potential [H4a] coupled with active uptake at heterotroph surfaces driven by 2) [H4b]. O_2 diffusion and active uptake is substrate- and population-specific, allowing [H4] to calculate lower O_2 concentrations at microbial surfaces associated with more biologically active substrates (e.g. manure). O_2 uptake by each heterotrophic population also accounts for competition for O_2 uptake with other heterotrophs, nitrifiers, roots and mycorrhizae,
4) DOC oxidation to CO_2 under ambient O_2 is calculated from 2) and 3) [H5]. The energy yield of DOC oxidation drives the uptake of additional DOC for construction of microbial biomass $M_{i,h}$ according to construction energy costs of each heterotrophic population [A21]. Energy costs of denitrifiers are slightly larger than those of obligately aerobic heterotrophs, placing denitrifiers at a competitive disadvantage for growth and hence DOC oxidation if e^- acceptors other than O_2 are not used.

Oxidation of DOC and Reduction of Nitrate, Nitrite and Nitrous Oxide by Denitrifiers

Constraints imposed by NO_3^- availability on DOC oxidation by denitrifiers are solved in five steps:

1) NO_3^- reduction to NO_2^- under non-limiting NO_3^- is calculated from electrons demanded by DOC oxidation but not accepted by O_2 because of diffusion limitations to O_2 supply, and hence transferred to NO_3^- [H6],
2) NO_3^- reduction to NO_2^- under ambient NO_3^- is calculated from 1), accounting for relative concentrations and affinities of NO_3^- and NO_2^- [H7],

3) NO_2^- reduction to N_2O under ambient NO_2^- is calculated from demand for electrons not met by NO_3^- in 2), accounting for relative concentrations and affinities of NO_2^- and N_2O [H8],

4) N_2O reduction to N_2 under ambient N_2O is calculated from demand for electrons not met by NO_2^- in 3) [H9],

5) additional DOC oxidation to CO_2 enabled by NO_x reduction in 2), 3) and 4) is added to that enabled by O_2 reduction from [H5], the energy yield of which drives additional DOC uptake for construction of $M_{i,n}$. This additional uptake offsets the disadvantage incurred by the larger construction energy costs of denitrifiers.

Oxidation of Ammonia and Reduction of Oxygen by Nitrifiers

Constraints on nitrifier oxidation of NH_3 imposed by O_2 uptake are solved in four steps:

1) substrate (NH_3) oxidation under non-limiting O_2 is calculated from active biomass, NH_3 and CO_2 concentrations, and an Arrhenius function of T_s [H11],

2) O_2 reduction to H_2O under non-limiting O_2 is calculated from 1) using set respiratory quotients [H12],

3) O_2 reduction to H_2O under ambient O_2 is calculated from radial O_2 diffusion through water films of thickness determined by soil water potential [H13a] coupled with active uptake at nitrifier surfaces driven by 2) [H13b]. O_2 uptake by nitrifiers also accounts for competition for O_2 uptake with heterotrophic DOC oxidizers, roots and mycorrhizae,

4) NH_3 oxidation to NO_2- under ambient O_2 is calculated from 2) and 3) [H14]. The energy yield of NH_3 oxidation drives the fixation of CO_2 for construction of microbial biomass $M_{i,n}$ according to construction energy costs of each nitrifier population.

Oxidation of Nitrite and Reduction of Oxygen by Nitrifiers

Constraints on nitrifier oxidation of NO_2^- to NO_3^- imposed by O_2 uptake [H15 - H18] are solved in the same way as are those of NH_3 [H11 - H14]. The energy yield of NO_2^- oxidation drives the fixation of CO_2 for construction of microbial biomass $M_{i,o}$ according to construction energy costs of each nitrifier population.

Oxidation of Ammonia and Reduction of Nitrite by Nitrifiers

Constraints on nitrifier oxidation imposed by NO_2^- availability are solved in three steps:

Biogeosciences Discuss., doi:10.5194/bg-2015-621, 2016
Manuscript under review for journal Biogeosciences
Published: 18 January 2016

1) NO_2^- reduction to N_2O under non-limiting NO_2^- is calculated from electrons demanded by NH_3 oxidation but not accepted by O_2 because of diffusion limitations to O_2 supply, and hence transferred to NO_2^- [H19],
2) NO_2^- reduction to N_2O under ambient NO_2^- and CO_2 is calculated from 1) [H20], competing for NO_2^- with [H8] and [H18],
3) additional NH_3 oxidation enabled by NO_2^- reduction in 2) [H21] is added to that enabled by O_2 reduction from [H14]. The energy yield from this oxidation drives the fixation of additional CO_2 for construction of $M_{i,n}$.

Uptake of Ammonium and Reduction of Oxygen by Roots and Mycorrhizae

1) NH_4^+ uptake by roots and mycorrhizae under non-limiting O_2 is calculated from mass flow and radial diffusion between adjacent roots and mycorrhizae [C23a] coupled with active uptake at root and mycorrhizal surfaces [C23b]. Active uptake is subject to inhibition by root nonstructural N:C ratios [C23g] where nonstructural N is the active uptake product, and nonstructural C is the CO_2 fixation product transferred from the canopy.
2) O_2 reduction to H_2O is calculated from 1) plus oxidation of root and mycorrhizal nonstructural C under non-limiting O_2 using set respiratory quotients [C14e],
3) O_2 reduction to H_2O under ambient O_2 is calculated from mass flow and radial diffusion between adjacent roots and mycorrhizae [C14d] coupled with active uptake at root and mycorrhizal surfaces driven by 2) [C14c]. O_2 uptake by roots and mycorrhizae also accounts for competition with O_2 uptake by heterotrophic DOC oxidizers, and autotrophic nitrifiers,
4) oxidation of root and mycorrhizal nonstructural C to CO_2 under ambient O_2 is calculated from 2) and 3) [C14b],
5) NH_4^+ uptake by roots and mycorrhizae under ambient O_2 is calculated from 1), 2), 3) and 4) [C23b].

Cation Exchange and Ion Pairing of Ammonium

A Gapon selectivity coefficient is used to solve cation exchange of NH_4^+ vs. Ca^{2+} [E10] as affected by other cations [E11] – [E15] and CEC [E16]. A solubility product is used to equilibrate soluble NH_4^+ and NH_3 [E24] as affected by pH [E25] and other solutes [E26 – E57].

Biogeosciences Discuss., doi:10.5194/bg-2015-621, 2016
Manuscript under review for journal Biogeosciences
Published: 18 January 2016

Soil Transport and Surface - Atmosphere Exchange of Gaseous Substrates and Products

Exchange of all modelled gases γ (γ = O_2, CO_2, CH_4, N_2, N_2O, NH_3 and H_2) between aqueous and gaseous states is driven by disequilibrium between aqueous and gaseous concentrations according to a T_s-dependent solubility coefficient, constrained by a transfer coefficient based on air-water interfacial area that depends on air-filled porosity [D14 – D15]. These gases undergo convective-dispersive transport through soil in gaseous [D16] and aqueous [D19] states driven by soil water flux and by gas concentration gradients. Dispersive transport is controlled by gaseous diffusion [D17] and aqueous dispersion [D20] coefficients calculated from gas- and water-filled porosity. Exchange of all gases between the atmosphere and both gaseous and aqueous states at the soil surface are driven by atmosphere - surface gas concentration differences and by boundary layer conductance above the soil surface, calculated from wind speed and from structure of vegetation and surface litter [D15].

FIELD EXPERIMENT

Site description

The Oensingen field site is located in the central Swiss lowlands (7° 44’E, 47° 17’N) at an altitude of 450 m. The climate is temperate with an average annual rainfall of about 1100 mm and a mean air temperature of 9.5 °C. The soil is classified as a Eutri-Stagnic Cambisol developed on clayey alluvial deposits, key properties of which are given in Table 1. Prior to the experiment, the field site was managed as a ley-arable rotation. In December 2000, the field was ploughed and left in fallow until 11 May 2001. The field was then sown with a grass-clover mixture typical for permanent grassland under intensive management. The field was ploughed again on 19 December 2007, left in fallow until 5 May 2008, when it was tilled and re-sown with the same grass-clover mix as in 2001. The period of study extended from sowing in 2001 to the end of 2009, during which the field was cut between three and five times per year and harvested as hay, silage or fresh grass, fertilized two to three times per year with manure as liquid cattle slurry and two to three times per year with mineral fertilizer as ammonium nitrate (NH_4NO_3) pellets, for an average annual N application of 23 g N m^{-2}. All key management operations during this period are summarized in Table 2.

Soil, plant and meteorological measurements

Biogeosciences Discuss., doi:10.5194/bg-2015-621, 2016
Manuscript under review for journal Biogeosciences
Published: 18 January 2016

Soil θ and T_s were recorded continuously using TDR (Time Domain Reflectometry, ThetaProbe ML2x, Delta-T Devices, Cambridge, UK) and thermocouples at 5, 10, 30 and 50 cm for θ and at 2, 5, 10, 30 and 50 cm for T_s. Leaf area index (LAI) was measured weekly with an optical leaf area meter (LI-2000, Li-Cor, Lincoln, NB, USA . Plants were collected every 2 to 4 weeks and the samples were dried for 48 h at 80°C, weighed and analyzed for C, N, P and K by using an elemental analyzer. Hourly climatic data were recorded continuously with an automated meteorological station, including air temperature (°C), rainfall (mm), relative humidity (%), global radiation (W m^{-2}) and windspeed (m s^{-1}).

Nitrous oxide flux measurements

N_2O fluxes were measured with a fully automated system consisting of up to eight stainless steel chambers (30 cm × 30 cm × 25 cm) (Flechard et al., 2005, Felber et al., 2014) fixed on PVC frames permanently inserted 10-cm deep into the soil. The positions of the chambers were changed about every two months. During measurements, the lids of the chambers were sequentially closed for 15 min. every 2 hours to allow N_2O accumulation in the chamber headspace. During closure the chamber atmosphere was recirculated at a rate of 1000 ml min.$^{-1}$ through polyamide tube lines (4-mm ID) to analytical instruments installed in a temperature-controlled field cabin adjacent to the field plots (10 m) and then back to the chamber headspace. Until autumn 2006 concentrations of N_2O, CO_2 and H_2O in the head space were measured once per minute with an INNOVA 1312 photoacoustic multi-gas analyzer (INNOVA Air Tech Instruments, Ballerup, Denmark; www.innova.dk). Interferences in the measurements caused by overlaps in the absorption spectra of the different gases and by temperature effects were corrected with a calibration algorithm described in detail by Flechard et al (2005). In autumn 2006 the system was changed to the gas filter correlation technique for N_2O (Model 46C, Thermo 279 Environmental Instruments Inc., Sunnyvale, CA, USA). This system was calibrated every 8 hours using certified standard gas mixtures (Messer Schweiz AG, Lenzburg, Switzerland) (Felber et al. 2014).

These measurements were used to calculate N_2O fluxes from the rate of change in concentration by using a linear or non-linear approach determined by the HMR R-package (Pedersen et al., 2010). The first three of the fifteen 1-min. measurements were omitted from the flux calculation to exclude gas exchange during closing that did not result from changes in emission/production in the soil. This procedure caused a mean increase of about 30% in the fluxes compared to values published in Fléchard et al. (2005) and Ammann et al. (2009), which were evaluated using linear regression Fluxes from all chambers were averaged over 4-hourly intervals and resulting values attributed to the mid-points of the intervals. Standard errors of these averages were calculated from all fluxes measured during each interval, and thus included both spatial and temporal variation. The fluxes measured from 2002 to 2003 were summarized in Fléchard et al. (2005). Those from 2004 to 2007 were re-evaluated from values described in Ammann et al. (2009). Those from 2008 and 2009 were reprocessed from the EU-Project NitroEurope-IP database using the HMR algorithm.

CO_2 and Energy Flux Measurements

CO_2 and energy fluxes were measured by an eddy covariance (EC) system consisting of three-axis sonic anemometers (models R2 and HS, Gill instruments, Lymington, UK) and an open-path infrared CO_2/H_2O gas analyzer (model LI-7500, Li-Cor, Lincoln, USA). The EC system used in this study is described in Ammann et al. (2007).

MODEL EXPERIMENT

Ecosys was initialized with the biological properties of plant functional types (PFTs) representing the ryegrass and clover planted at Oensingen. These properties were identical to those in an earlier study (Grant et al., 2012) except for a perennial rather than annual growth habit. These PFTs competed for common resources of radiation, water and nutrients, based on their vertical distributions of leaf area and root length driven by C fixation and allocation in each PFT. *Ecosys* was also initialized with the physical and chemical properties of the Eutri-Stagnic Cambisol at Oensingen (Table 1). The model was then run from model dates 1 Jan. 1931 to 31 Dec. 2000 under repeating sequences of land management practices and continuous hourly weather data (radiation, T_a, RH, wind speed and precipitation) recorded at Oensingen from 1 Jan. 2001 to 31 Dec. 2007 (i.e. 10 cycles of 7 years). This run was long enough for C, N and energy cycles in the model to attain equilibrium under the Oensingen site conditions well before the end of the spinup run. The modelled site was plowed on 19 Dec. 2000, terminating all PFTs.

Biogeosciences Discuss., doi:10.5194/bg-2015-621, 2016
Manuscript under review for journal Biogeosciences
Published: 18 January 2016

The model run was then continued from model dates 1 Jan. 2001 to 31 Dec. 2009 under continuous hourly weather data recorded at Oensingen from 1 Jan. 2001 to 31 Dec. 2009 with the same PFTs and land management practices as those at the field site listed in Table 2. For each manure application in the model, an irrigation of 4 mm was added to account for the water in the slurry. For each harvest in the model, the fraction of canopy LAI to be cut (usually 0.85 – 0.95) was calculated from measurements of LAI before and after the corresponding harvest in the field. In *ecosys*, canopy leaves are dynamically resolved into a selected number of layers (10 in this case) of equal LAI. The leaf area to be cut was removed from successive leaf layers from the top of the combined canopy downwards so that the LAI cut from each PFT depended on the leaf area of the PFT in these layers. Of the phytomass cut with the LAI, a fraction of 0.76 was removed as harvest and the remainder was added to surface litter, as determined in the intensively managed grassland at Oensingen by Amman et al. (2009). N_2O emissions modelled from 2004 through 2009 were compared with those measured by the automated chambers. These comparisons were supported by ones with thermistor and TDR measurements of T_s, θ, and with EC measurements of CO_2 and energy exchange.

To examine the possible effects of different land management practices on N_2O emissions, the model run from 2001 to 2009 (field) was repeated with (1) increased harvest intensity in which canopy LAI remaining after each harvest was reduced to one-half of those in the first run (1/2), and (2) increased harvest intensity with each harvest delayed by 5 days (1/2 + 5d). These alternative practices caused canopy regrowth to be slower during emission events following subsequent manure and fertilizer applications.

RESULTS

LAI Modelled vs. Measured from 2002 to 2009

Accurate modelling of ecosystem C cycling and hence N_2O emissions requires accurate modelling of plant growth as determined by land management practices. LAI modelled and measured from 2002 to 2009 rose rapidly from low values remaining in spring and after each harvest (Table 1) to 4 – 6 m^2 m^{-2} before the next harvest, except during 2003 (Fig. 1). Regrowth of LAI in *ecosys* was driven by nonstructural C, N and P pools replenished partly from storage reserves after harvests, but mostly from products of current C, N and P uptake. Replenishment had to proceed rapidly to sustain

Biogeosciences Discuss., doi:10.5194/bg-2015-621, 2016
Manuscript under review for journal Biogeosciences
Published: 18 January 2016

the rapid rates of regrowth observed in the field. Regrowth of LAI in the model was less than that measured in 2009 because more frequent cutting slowed replenishment.

Daily-Aggregated N_2O Fluxes Modelled vs. Measured from 2004 to 2009

Daily aggregations of both measured and modelled N_2O emissions indicated that emission events during the study period were confined to intervals of no longer than 5 days when precipitation followed manure or fertilizer applications (Fig. 2). Outside of these intervals emissions remained very small except for a period of emissions modelled, but not measured, after manure application in autumn 2006 (Fig. 2c) and measured, but not modelled, before fertilizer application in spring 2008 (Fig. 2e). The largest emissions followed manure applications in July and August, but their magnitudes did not vary with the amount of manure N applied. For example, emissions during an event in August 2009 (239 vs. 184 mg N m^{-2} measured vs. modelled in Fig. 2f) were greater than those during an event in July 2007 (83 vs. 112 mg N m^{-2} measured vs. modelled in Fig. 2d) which in turn were greater than those during an event in July 2005 (48 vs. 79 mg N m^{-2} measured vs. modelled in Fig.2b), but manure N application preceding the event in August 2009 was less than that in July 2007 which in turn was less than that in July 2005 (Table 2). The magnitude of emission events following fertilizer application also varied. For example, emissions during an event in late August 2007 (105 vs. 82 mg N m^{-2} measured vs. modelled in Fig. 2d) were greater than those during events in September 2004 and 2005 (10 vs. 3 mg N m^{-2} measured vs. modelled in Fig 2a, and 4 vs. 7 mg N m^{-2} measured vs. modelled in Fig. 2b), although the fertilizer N applications preceding each event were the same (Table 2). These differences in emissions indicated differences in ecological controls imposed by environmental conditions (θ and T_s) and plant management during each event. Uncertainty in the measured events was estimated to be ~30% of their values.

Relationships between N_2O Fluxes and Environmental Conditions during Emission Events

Environmental conditions measured and modelled from harvest to the end of the two largest emission events following manure applications in July 2007 (Fig. 2d) and August 2009 (Fig.2f) were examined in greater detail to investigate relationships among near-surface T_s, θ, aqueous gas concentrations, and surface fluxes of energy, CO_2 and N_2O (Figs. 3 and 4). In July 2007, several small precipitation events wetted and cooled the soil between harvesting on DOY 187 and manure application on DOY 194 (Fig. 3a,b). The soil then dried during several days without precipitation and warmed with reduced shading from defoliation (Fig. 1) until DOY 200, after which the soil wetted with further precipitation and cooled with increased shading from plant regrowth (Fig. 3a,b). The higher θ measured during this period (Fig. 3b) may have been caused by difficulties in maintaining calibration of the TDR probes over long periods in the high-clay soil at Oensingen (Table 1). This higher θ was not likely caused by overestimated evapotranspiration because modelled LE fluxes, reduced by low LAI after harvesting but increasing with subsequent regrowth, were close to those measured (Fig. 3c), suggesting that total water uptake was accurately modelled. Comparison of modelled and measured θ was further complicated by soil cracking which altered infiltration at low θ.

CO_2 influxes were also reduced by low LAI after cutting, but recovered to pre-cut levels by the end of the emission event (Fig. 3d), driving rapid regrowth of LAI (Fig. 1). Influxes measured in the field were reduced from those in the model for several days after manure application, suggesting temporary interference of CO_2 fixation by the application.

Litterfall from plant growth [C18, C19] and cutting, as well as manure application caused a litter layer of 1 – 2 cm to develop on the soil surface in the model. During the N_2O emission event from DOY 200 to DOY 205 in 2007 (Fig. 2d), several precipitation events (Fig. 3a) wetted the modelled surface litter and near-surface soil (layers 1 and 2 in Table 1) (Fig. 3e) without increasing θ at 5 cm (Fig. 3b). This surface wetting sharply reduced aqueous O_2 concentrations $[O_{2(s)}]$ (Fig. 3f) and thereby raised aqueous N_2O concentrations $[N_2O_{(s)}]$ (Fig. 3g). Between precipitation events, drying of the surface litter and near-surface soil in the model allowed recovery of $[O_{2(s)}]$ and forced declines in $[N2O_{(s)}]$. These rises and declines in $[N2O_{(s)}]$ drove rises and declines in N_2O emissions that tracked those measured in the chambers (Fig. 3h). These emissions rose immediately with the onset of precipitation on DOY 200 (Fig. 3a) before wetting at 5 cm (Fig. 3b), indicating that emissions were driven by surface wetting (Fig. 3e). The net generation of N_2O modelled in each soil zone, calculated from [H8] + [H20] – [H9], indicated that 0.21 of surface emissions originated in the surface litter and the remainder in the 0 – 1 cm soil layer as indicated by higher $[N_2O_{(s)}]$ (Fig. 3g), while the deeper soil layers were a very small net sink of N_2O. Rises and declines in $[N_2O_{(s)}]$ also drove rises and declines in N_2 emissions that persisted until DOY 205, after which more rapid mineral N uptake with recovering plant growth, driven by rising CO_2 influxes (Fig. 3d), caused both emissions to return to background levels (Fig. 3h).

In 2009, a period of low precipitation with soil drying and warming occurred between harvesting in late July and manure application on DOY 218 in early August, followed by heavy precipitation with soil wetting and cooling on DOY 220 (Fig. 4a,b). LE effluxes and CO_2 influxes declined sharply with LAI after cutting, and did not recover to pre-cut levels by the end of the subsequent emission event on DOY 224 (Fig. 4c,d). Slurry application caused brief surface wetting on DOY 218 (Fig. 4e) and heavy precipitation on DOY 220 caused prolonged soil wetting at the surface (Fig. 4e) and at 5 cm (Fig. 4b). Wetting caused declines in $[O_{2(s)}]$ (Fig. 4f) and thereby rises in $[N_2O_{(s)}]$ (Fig. 4g) sustained over 3 days. These rises drove particularly rapid N_2O emissions in the model which were consistent in magnitude with those measured in the chambers (Fig. 4h). Diurnal variation modelled with soil warming and cooling (Fig. 4a) was not apparent in the measurements, although modelled values remained within the large uncertainty of the measured values during the emission event. These large emissions were enabled in the model by slow plant uptake of manure N (Table 2) caused by the slow recovery of plant CO_2 uptake and hence growth after cutting (Fig. 4d). The rises in $[N_2O_{(s)}]$ also drove rises in modelled N_2 emissions (Fig. 4h). Emissions declined with surface litter drying on DOY 223 (Fig. 4e) which allowed surface $[O_{2(s)}]$ to rise (Fig. 4f) and $[N_2O_{(s)}]$ to fall (Fig. 4g), while θ at 5 cm remained high (Fig. 4b), again indicating that litter was an important source of N_2O. The net generation of N_2O modelled in each soil zone indicated that 0.48 of surface emissions originated in the surface litter, 0.48 in the 0 – 1 cm soil layer and 0.05 in the 1 – 3 cm soil layer, while the deeper soil layers were a very small net sink of N_2O, as indicated by near-surface gradients of $[N_2O_{(s)}]$ (Fig. 4g).

Greater N_2O emissions were modelled and measured during the event in August 2009 vs. July 2007 (Fig. 4h vs. Fig. 3h), in spite of smaller N addition (Fig. 2f vs. Fig. 2d; Table 2) and similar θ and T_s modelled and measured at 5 cm (Fig. 4a,b vs. Fig. 3a,b). These greater emissions were attributed in the model to (1) earlier and heavier precipitation after manure application (2 days after application in Fig. 4a vs. 6 days in Fig. 3a), and (2) slower recovery of CO_2 fixation after defoliation, indicated by slower rises in diurnal amplitude of CO_2 fluxes (Fig. 4d vs. Fig. 3d). Heavier precipitation in 2009 vs. 2007 drove sustained vs. intermittent surface and near-surface wetting (Fig. 4e vs. Fig. 3e) and hence sustained vs. intermittent declines in $[O_{2(s)}]$ and rises in $[N_2O_{(s)}]$ (Fig. 4f,g vs. Fig. 3f,g). Slower recovery of CO_2 fixation after cutting in 2009 vs. 2007 slowed removal of added

Biogeosciences Discuss., doi:10.5194/bg-2015-621, 2016
Manuscript under review for journal Biogeosciences
Published: 18 January 2016

NH_4^+ and NO_3^- from soil. This slower removal, combined with the shorter period between manure application and precipitation, left larger NO_3^- concentrations ($[NO_3^-]$) in litter and surface soil to drive N_2O production following precipitation [H7]. These model findings indicated the importance to N_2O emissions of surface and near-surface θ after precipitation, and of plant management (intensity and timing of defoliation in relation to N application) and its effect on subsequent CO_2 fixation.

Effects of Intensity and Timing of Defoliation on N_2O Emission Events

Increasing harvest intensity and delaying harvest dates slowed LAI regrowth modelled during emission events following manure or fertilizer applications (Fig. 5). The effects of this slowing on N_2O emissions were examined during emission events modelled under diverse θ and T_s (Figs. 6, 7). Slower LAI regrowth from increasing and delaying defoliation following manure application on DOY 194 in 2006 (Table 2) slowed the recovery of CO_2 fixation (Fig. 6a) and of NH_4^+ uptake (Fig. 6b), allowing more nitrification of manure N and hence greater surface $[NO_3^-]$ (Fig. 6c). Slower LAI regrowth (Fig. 5) also reduced shading and ET, raising T_s (Fig. 6d) and θ (Fig. 6e). N_2O emissions modelled under field management remained small because of soil drying, in spite of high T_s, consistent with measurements (Fig. 6f). Increases in emissions modelled with slower LAI regrowth, particularly from delayed harvesting (Fig. 6f), were attributed to slower N uptake (Fig. 6b) and hence larger $[NO_3^-]$ in litter and surface soil (Fig. 6c), and to warmer and wetter soil (Fig. 6d,e) which increased O_2 demand while reducing O_2 supply.

Slower LAI regrowth from increasing and delaying defoliation following a similar manure application on DOY 194 in 2007 (Table 2; Fig. 5) also caused reductions in CO_2 fixation (Fig. 6g), which slowed NH_4^+ and NO_3^- uptake (Fig. 6h), allowing more nitrification of manure N and hence greater $[NO_3^-]$ (Fig. 6i). Lower LAI also caused increases in T_s (Fig. 6j) and θ (Fig. 6k). Emissions modelled and measured under field management in 2007 (Fig. 6l) were greater than those in 2006 (Fig. 6f), in spite of lower T_s (Fig. 6j vs. 6d), because near-surface wetting from several precipitation events (Fig. 3e) reduced $[O_{2(s)}]$ and increased $[N_2O_{(s)}]$ (Fig. 3f,g). Emissions modelled with increased and delayed harvesting rose from those with field harvesting as the emission event progressed (Fig. 6l) because elevated $[NO_3^-]$ from the manure application persisted longer during the event (Fig. 6i).

Biogeosciences Discuss., doi:10.5194/bg-2015-621, 2016
Manuscript under review for journal Biogeosciences
Published: 18 January 2016

Emissions modelled and measured following fertilizer application on DOY 259 in 2005 (Table 2) remained small after soil wetting (Fig. 7f) because lower T_s (Fig. 7d) slowed soil respiration after wetting, manifested as smaller measured and modelled CO_2 effluxes (Fig. 7a), and so slowed demand for e^- acceptors. Under these conditions, increasing and delaying defoliation had little effect on modelled N_2O emissions (Fig. 7f), while CO_2 fixation (Fig. 7a) and N uptake (Fig. 7b) were only slightly reduced and surface NO_3^- only slightly increased (Fig. 7c). Emissions modelled and measured following the same fertilizer application on DOY 240 in 2007 (Fig. 7l) were greater than those in 2005 because soils were warmer (Fig. 7j) with more rapid respiration (Fig. 7g), and because fertilizer application and subsequent wetting occurred sooner after cutting (Table 2). Consequently recovery of CO_2 fixation was less advanced (Fig. 7g), reducing cumulative N uptake (Fig. 7h) and leaving larger [NO_3^-] to drive N_2O generation during the event (Fig. 7h). However reducing LAI remaining after each harvest did not raise N_2O emissions after this application (Fig. 7l), because slower LAI regrowth caused declines in primary productivity and consequently litterfall, so that later in the year surface litter sometimes declined to levels at which N_2O generation modelled in the litter was reduced.

Effects of Defoliation Intensity and Timing on Annual Productivity and N_2O Emissions

In the model, plant management practices affected LAI regrowth (Fig. 5), CO_2 fixation, N uptake, and hence soil [NO_3^-] and N_2O emissions (Figs. 6, 7). These effects were summarized at an annual time scale in Table 3. Modelled and EC-derived gross primary productivity (GPP) remained close to 2000 g C m^{-2} y^{-1} during most years except with low precipitation in 2003 and replanting in 2008, indicating a highly productive ecosystem with rapid C cycling and hence demand for e^- acceptors (Table 3). Larger modelled vs. measured GPP caused larger modelled vs. measured NEP in 2003, 2005 and 2007. Harvest removals in the model varied with NEP except during replanting in 2008, but tended to exceed those recorded in the field, particularly with low EC-derived NEP in 2005 and 2006. Modelled values were determined in part by the assumed constant harvest efficiency of 0.76. Including C inputs from manure applications, modelled and estimated net biome productivity (NBP) were positive except during replanting in 2008, indicating that this intensively managed grassland is a C sink unless replanted. Average annual NBP modelled vs. measured from 2002 to 2009 was 30 vs. 58 g C m^{-2}, with the lower modelled value attributed to greater modelled harvest removals, particularly in 2006.

Biogeosciences Discuss., doi:10.5194/bg-2015-621, 2016
Manuscript under review for journal Biogeosciences
Published: 18 January 2016

Slower LAI regrowth from increasing and delaying defoliation (Fig. 5) reduced modelled GPP, R_e and hence NEP by 5 - 10% during years with greater productivity. However increasing and delaying defoliation did not much affect harvest removals because reduced NEP was offset by greater harvest intensity, so that NBP was reduced except with replanting in 2008.

Annual N_2O emissions were estimated from chamber measurements for each year of the study by scaling the mean measured fluxes to annual values. These values are presented in Table 3 as upper boundaries for annual emissions because flux measurements from which means were calculated were more frequent during emission events. A lower boundary for annual emissions was also estimated in Table 3 by replacing missing flux measurements with zero. Average lower and upper boundaries for annual emissions estimated from 2002 to 2009 were 220 and 355 g N m^{-2} respectively vs. an average annual emission in the model of 0.260 g N m^{-2} (Table 3). Modelled emissions were larger than the range of estimated values in 2006 when no significant emission events were measured even with relatively high precipitation (Fig. 2c), and smaller in 2008 and 2009 when measured values were particularly large in spite of smaller N inputs. Annual emissions in the model were close to 1% of annual N inputs during most years, but were more in 2008 and 2009 with the large emission events following summer applications of fertilizer and manure (Fig. 2e,f). Annual N inputs (Table 3), supplemented by 3 – 6 g N m^{-2} y^{-1} modelled from symbiotic fixation by clover [F1 – F26]), were only slightly larger than annual N removals with harvesting, plus 2 – 3 g N m^{-2} y^{-1} lost from all other gaseous and aqueous emissions (N_2 from denitrification, NH_3 from volatilization, NO_3^- from leaching). Consequently residual soil NO_3^-, while present in the model, did not accumulate during the study period, and so did not drive increasing N_2O emissions with sustained N applications. Modelled and measured annual N_2O emissions, if expressed in C equivalents (~130 g C g N^{-1}), largely offset net C uptake expressed as NBP.

Increasing harvest intensity and delaying harvest dates had little effect on annual N_2O emissions modelled during the first two years after planting in 2001 and 2008, but raised them substantially thereafter (2003 – 2007) (Table 3). During this period, annual emissions rose by an average of 24% with increased harvest intensity, and by an average of 43% with increased harvest intensity and delayed harvest dates. These increases were attributed to reduced N uptake, and to increased T_s and θ (Figs. 6, 7).

DISCUSSION

Modelled vs. Measured N_2O Emissions

Most N_2O emission events measured from 2004 to 2009 were simulated within the range of measurement uncertainty, estimated to be about 30% of mean values (Fig. 2). However some deviations between modelled and measured N_2O emissions were apparent, such as the larger emissions modelled in autumn 2006 (Fig. 2c) and the smaller emissions modelled in spring 2008 (Fig. 2e). These deviations may be attributed to uncertainties in both the measurements and the model. In the automated measurement system, the static chambers were rotated about every two months among fixed positions in a corner of the field. During these periods, surface conditions in the chamber could deviate from the mean field conditions represented in the model. However we do not have an explanation for the very small emissions measured after the three manure slurry applications 2006. The chambers had been removed before the applications and were reinstalled within two hours, during which the cut grass was removed so that the surface litter in the chambers may have been reduced from that outside. In the model, emissions following manure or fertilizer applications were sensitive to the amount of surface litter as noted earlier. The absence of emission events measured after slurry applications in 2006 was unusual (Fig. 2), demonstrating that large small-scale spatial variability inevitably affects these measurements.

During spring 2008 sustained emissions of about 5 mg N m^{-2} d^{-1} were measured by the chambers in the absence of any manure or fertilizer applications (Fig. 2e). These emissions were related to the ploughing of the field to a depth of 25cm in December 2007 (Table 2) which hastened soil organic matter decomposition, and hence N mineralization that increased mineral N substrate for nitrification and denitrification, and possibly microbial nitrifier and denitrifier populations. These increases must remain hypothetical as the Oensingen study did not include stratified analysis of N_2O production parameters (e.g. microbial biomass, potential denitrification) within the chamber soils. Although *ecosys* simulates hastened SOM decomposition with tillage (Grant et al., 1998), large amounts of above- and below-ground plant litter with relatively high C:N ratios were incorporated in the model with tillage in December 2007 which slowed net N mineralization and hence accumulation

Biogeosciences Discuss., doi:10.5194/bg-2015-621, 2016
Manuscript under review for journal Biogeosciences
Published: 18 January 2016

of mineral N products in the model during spring 2008. Consequently modelled N_2O emissions remained small until mineral N was raised by fertilizer applications in July (Fig. 2c).

Modelling Controls on N_2O Emissions by Litter and Near-Surface θ and T_s

In the model, almost all the N_2O emissions originated in the surface litter and in the near-surface (0 – 1 cm) soil layer, so that emissions were strongly controlled by litter and near-surface θ and T_s (Figs. 3 – 4). This model finding is consistent with the experimental finding of Pal et al. (2013) from ^{15}N enrichment studies that approximately 70% of N_2O measured during emission events in a managed grassland originated in the surface litter. Similarly van der Weerden et al. (2013) inferred from diurnal variation in T_s and N_2O emissions measured after urine amendments on a managed grassland that N_2O production was at or near the soil surface (0 - 2 cm). Also Fléchard et al. (2007) inferred in a meta-analysis of N_2O emissions from grasslands in Europe that θ measured at 5 cm was not in some cases an adequate scaling factor for N_2O source strength because N_2O production and emission took place at or near the soil surface. *Ecosys* simulated little net production, and even a small net consumption, of N_2O below 2 cm during emission events, as may be inferred from peak $[N_2O_{(s)}]$ modelled in the 0 – 1 cm soil layer and much lower $[N_2O_{(s)}]$ modelled in the 1 – 3 cm soil layer below (Figs. 3g and 4g). This model finding was consistent with the experimental finding of Neftel et al. (2000) that N_2O concentrations below near-surface soil layers in a managed grassland remained below atmospheric values during emission events, indicating that any N_2O generated at depths greater than ~3 cm would not likely reach the soil surface. Thus attempts to relate N_2O emissions to T_s and θ measured at greater depths than 3 cm are unlikely to be informative if these differ from near-surface values.

Consequently modelled N_2O emissions were highly sensitive to surface wetting and drying (e.g. Fig. 3e,h) modelled from precipitation vs. ET (e.g. Fig. 3a,c), or to surface warming and cooling (e.g. Fig. 7i,l) modelled from surface energy balance (e.g. Fig. 3a,c). The sensitivity to surface wetting and drying was modelled from the effects of θ on air- vs. water-filled porosity and hence on diffusivity of gases in gaseous [D17] and aqueous [D20] phases, and on gaseous volatilization - dissolution transfer coefficients and hence gas exchange between gaseous and aqueous phases [D14, D15]. These transfers controlled O_2 supply, and hence demand for alternative e^- acceptors as the O_2 supply fell below O_2 demand, which drove N_2O generation from denitrification [H6 – H8] and nitrification

Biogeosciences Discuss., doi:10.5194/bg-2015-621, 2016
Manuscript under review for journal Biogeosciences
Published: 18 January 2016

[H19]. The control of O_2 supply on e^- acceptors used in nitrification thereby simulated the effect of WFPS on the fraction of N_2O generated during nitrification identified by Fang et al. (2015) as necessary to modelling N_2O emissions, while avoiding model-specific parameterization. The sensitivity to surface wetting in *ecosys* enabled sharp rises in N_2O emissions to be modelled from surface litter and near-surface soil after small precipitation events during DOY 200 - 201 in 2007 (Fig. 3a,h), and after slurry application during DOY 218 in 2009 (Fig. 4a,h), even when the soil at 5 cm remained dry (Fig. 3b; Fig. 4b). Such rises were consistent with the experimental findings of Fléchard et al. (2007) that precipitation on dry soil can cause substantial N_2O emissions after fertilizer application in grasslands.

The sensitivity to surface warming and cooling was modelled from the effects of T_s on diffusivity of gases in gaseous [D17] and aqueous [D20] phases, and on gaseous solubility and hence gas exchange between gaseous and aqueous phases [D14, D15], both parameterized independently from the model. These transfers controlled [$O_{2(s)}$] in the surface litter and soil (Figs. 3f and 4f), and hence O_2 uptake by aerobic heterotrophs [H4] and autotrophs [H13] through a Michaelis-Menten constant [H4b, H13b]. The sensitivity to surface warming and cooling was also modelled from the effects of T_s on SOC oxidation [H2] and hence O_2 demand by aerobic heterotrophs [H3], and on NH_4^+ and NO_2^- oxidation [H11, H15] and hence O_2 demand by aerobic autotrophs [H12, H16]. These effects were driven by a single Arrhenius function [A6] parameterized independently from the model. Under sustained high surface θ, diurnal surface warming and cooling could drive large diurnal variation in N_2O emissions (e.g. DOY 221 in Fig. 4h, DOY 243 in Fig. 7l) as observed by van der Weerden et al. (2013), although under variable surface θ this variation was dominated by that from surface wetting and drying (e.g. Figs. 3h, 6l). At a seasonal time scale, higher T_s could cause large increases in N_2O emissions modelled with comparable θ after the same fertilizer application (Fig. 7l vs. Fig. 7f).

Values of both θ and T_s thus determined O_2 demand not met by O_2 uptake which drove demand for alternative e^- acceptors by heterotrophic denitrifiers [H6] and autotrophic nitrifiers [H19]. This demand drove the sequential reduction of NO_3^-, NO_2^- and N_2O to NO_2^-, N_2O and N_2 respectively by heterotrophic denitrifiers [H7, H8, H9], and the reduction of NO_2^- to N_2O by autotrophic nitrifiers

Biogeosciences Discuss., doi:10.5194/bg-2015-621, 2016
Manuscript under review for journal Biogeosciences
Published: 18 January 2016

[H20]. The consequent production of N_2O (Figs.3g, 4g) and N_2 drove emissions (Fig. 3h, 4h) through volatilization [D14, D15] and through gaseous and aqueous diffusion [D16, D19].

Ratios of N_2O and N_2 emissions in *ecosys* (Figs. 3h, 4h) were not parameterized as done in other models, but rather were determined by environmental conditions. When demand from heterotrophic denitrifiers for alternative e^- acceptors was small relative to their availability, the preferential reduction of more oxidized e^- acceptors generated larger emissions of N_2O [H7, H8] relative to N_2 [H9]. Such conditions occurred during the early part of an emission event when surface [NO_3^-] rose with nitrification of fertilizer or manure NH_4^+ after application (e.g. DOY 200 – 201 in Fig. 3h). However when demand for alternative e^- acceptors was large relative to their availability, this same reduction sequence forced more rapid reduction of N_2O to N_2 and hence smaller emissions of N_2O relative to N_2. Such conditions occurred during the later part of emission events when surface [NO_3^-] declined with plant uptake (e.g. DOY 202 – 205 in Fig. 3h and DOY 222 in Fig. 4h), or when greater surface wetting reduced O_2 supply (e.g. DOY 220 in Fig. 4h). This greater demand for alternative e^- acceptors with wetting provided a process-based explanation for declines in N_2O emissions frequently found at higher θ in field studies (e.g. Rafique et al., 2011).

Nitrification and denitrification were also driven by the concentrations of NH_4^+ [H11], NO_3^- [H7], NO_2^- [H8, H15, H20] and N_2O [H9] relative to Michaelis-Menten constants. The concentrations of NH_4^+ and NO_3^- in *ecosys* were increased by N additions from manure and fertilizer N applications (Table 2), and by net mineralization soil organic N from oxidation of litterfall, manure and SOM [A26] as indicated by soil CO_2 effluxes. Concentrations were reduced by root uptake of NH_4^+ and NO_3^- [C23] and consequent plant N assimilation with growth, indicated by more rapid CO_2 fixation with time after cutting (Figs 3 – 4 and Figs. 6 - 7). In the model, more rapid CO_2 fixation drove more rapid production of nonstructural C, and hence more rapid exchange of nonstructural C and N between canopy and roots [C50], and so hastened root active N uptake by increasing R_a driving root growth [C14b], and by hastening removal of N uptake products and hence reducing their inhibition of active uptake [C23g].

Modelling Effects of Defoliation Intensity and Timing on N_2O Emissions

Biogeosciences Discuss., doi:10.5194/bg-2015-621, 2016
Manuscript under review for journal Biogeosciences
Published: 18 January 2016

The control of NH_4^+ and NO_3^- availability by root N uptake indicated that plant management practices determining uptake would thereby affect N_2O emissions. In the model, increasing harvest intensity and delaying harvest dates both slowed N uptake (Fig. 6b,h and Fig. 7b,h) by slowing the recovery of LAI (Fig. 5) and CO_2 fixation (Fig. 6a,g and Fig. 7a,g). Both thereby increased $[NO_3^-]$ (Fig. 6c,i and Fig. 7c,i), T_s (Fig. 6d,j and Fig. 7d,j) and θ (Fig. 6e,k and Fig. 7e,k), raising N_2O effluxes modelled during most emission events (Fig. 6f,l and Fig. 7f,l), and hence annually (Table 3). This model finding was consistent with the field observations of Jackson et al. (2015) that increased N_2O emissions after defoliation in grasslands were caused by reduced uptake of N and water by slower-growing plants.

The effects of defoliation on N_2O emissions during modelled emission events were similar to, or greater than, those of T_s and θ (e.g. Fig. 6f,l), consistent with the experimental finding of Imer et al. (2013) that plant management, as represented by its effects on LAI, had a larger effect on N_2O fluxes than did the environment, as represented by T_a, at an intensively managed grassland in Switzerland. Reducing LAI remaining after harvest by one-half and delaying harvest by 5 days had little effect on modelled harvest removals (Table 3), suggesting that N_2O emissions from managed grasslands are more sensitive to plant management practices than are yields. Intensity and timing of harvests should therefore be selected to avoid slow regrowth of LAI following N additions by avoiding excessive defoliation and by allowing as much time as possible between defoliation and subsequent fertilizer or manure application. Neftel et al. (2010) reported enhanced N_2O emissions after cuts in managed grassland and hypothesized that a simple mitigation option would be to optimize the timing of the fertilizer applications. To our knowledge this option has not been systematically investigated, but may have been considered by environmentally concerned farmers.

CONCLUSIONS

N_2O emissions modelled in this managed grassland originated in the surface litter and upper 2 cm of the soil profile. The shallow origin of these emissions enabled *ecosys* to simulate the response of measured emissions to changes in near-surface θ and T_s during brief emission events when rainfall followed manure or mineral fertilizer applications. Measurements of θ and T_s used to estimate N_2O

Biogeosciences Discuss., doi:10.5194/bg-2015-621, 2016
Manuscript under review for journal Biogeosciences
Published: 18 January 2016

emissions from managed grasslands should therefore be taken in surface litter and near-surface soil (0 – 2 cm), rather than deeper in the soil profile (5 – 10 cm) as is currently done.

N_2O fluxes modelled during emission events were greater when grassland regrowth and hence mineral N uptake was slower following harvest and subsequent N application. The control of N_2O emissions by grassland N uptake indicated that N_2O emissions from managed grassland could be increased by harvesting practices and fertilizer timing that resulted in slower regrowth during periods when emission events are most likely to occur.

ACKNOWLEDGEMENTS

Computational facilities for *ecosys* were provided by the University of Alberta and by the Compute Canada high performance computing infrastructure. A PC version of *ecosys* with GUI can be obtained by contacting the corresponding author at rgrant@ualberta.ca.

Biogeosciences Discuss., doi:10.5194/bg-2015-621, 2016
Manuscript under review for journal Biogeosciences
Published: 18 January 2016

REFERENCES

Ammann, C., Fléchard, C., Leifeld, J., Neftel, A. and Fuhrer, J.:. The carbon budget of newly established temperate grassland depends on management intensity. Agriculture, Ecosystems and Environment 121, 5–20, 2007

Ammann, C., Spirig, C., Leifeld, J. and Neftel, A.: Assessment of the nitrogen and carbon budget of two managed temperate grassland fields. Agriculture, Ecosystems and Environment 133, 150–162, 2009

Chatskikh, D.D., Olesen, J.E., Berntsen, J., Regina, K. and Yamulki, S.: Simulation of effects of soils, climate and management on N_2O emission from grasslands, Biogeochem. 76, 395-419, 2005

Craswell, E. T.: Some factors influencing denitrification and nitrogen immobilization in a clay soil, Soil Biol. Biochem. 10, 241-245, 1978

Fang, Q.X., Ma, L., Halvorson, A.D., Malone, R.W., Ahuja, L.R., Del Grosso, S.J. and Hatfield, J.L.: Evaluating four nitrous oxide emission algorithms in response to N rate on an irrigated corn field. Environmental Modelling & Software 72, 56-70, 2015.

Felber, R., Leifeld, J., Horak J and Neftel, A.: Nitrous oxide emission reduction with greenwaste biochar: comparison of laboratory and field experiments European Journal of Soil Science 65, 128–138 doi: 10.1111/ejss.12093, 2014.

Fléchard, C.R., Neftel, A., Jocher, M., Ammann, C. and Fuhrer, J.: Bi-directional soil/atmosphere N_2O exchange over two mown grassland systems with contrasting management practices. Glob Change Biol 11, 2114–2127, 2005.

Fléchard, C.R., Ambus, P., Skiba, U., Rees, R.M., Hensen, A., van Amstel, A., van den Pol-van Dasselaar, A., Soussana, J.-F., Jones, M., Clifton-Brown, J., Raschi, A., Horvath, L., Neftel, A., Jocher, M., Ammann, C., Leifeld, J., Fuhrer, J., Calanca, P., Thalman, E., Pilegaard, K., Di Marco, C., Campbell, C., Nemitz, E., Hargreaves, K.J., Levy, P.E., Ball, B.C., Jones, S.K., van de Bulk, W.C.M., Groot, T., Blom, M., Domingues, R., Kasper, G., Allard, V., Ceschia, E., Cellier, P., Laville, P., Henault, C., Bizouard, F., Abdalla, M., Williams, M., Baronti, S., Berretti F. and Grosz, B.: Effects of climate and management intensity on nitrous oxide emissions in grassland systems across Europe, Agric. Ecosyst. Environ. 121, 135-152, 2007.

Conant, R.T, Paustian, K., Del Grosso, S.J. and Parton, W.J.: Nitrogen pools and fluxes in grassland soils sequestering carbon. Nutr Cycl Agroecosyst 71, 239–248, 2005.

Grant, R.F."A review of the Canadian ecosystem model *ecosys*. pp. 173-264 in: *Modeling Carbon and Nitrogen Dynamics for Soil Management*. Shaffer M. (ed). CRC Press. Boca Raton, F, 2001.

Grant, R.F., Juma, N.G. and McGill, W.B.: Simulation of carbon and nitrogen transformations in soils. I. Mineralization. Soil Biol. Biochem. 27, 1317-1329, 1993a

Grant, R.F., Juma, N.G. and McGill, W.B.: Simulation of carbon and nitrogen transformations in soils. II. Microbial biomass and metabolic products. Soil Biol. Biochem. 27,1331-1338, 1993b

Grant, R.F., Izaurralde, R.C., Nyborg, M., Malhi, S.S., Solberg, E. D. and Jans-Hammermeister, D.: Modelling tillage and surface residue effects on soil C storage under current vs. elevated CO_2 and temperature in *ecosys* pp. 527-547 in *Soil Processes and the Carbon Cycle*. Lal, R., Kimble J.M., Follet, R.F. and Stewart, B.A.(eds). CRC Press. Boca Raton, FL, 1998.

Grant, R.F. and Pattey, E.: Mathematical modelling of nitrous oxide emissions from an agricultural field during spring thaw. Global Biogeochem. Cycles. 13, 679-694, 1999

Grant, R.F. and Pattey E.: Modelling variability in N_2O emissions from fertilized agricultural fields. Soil Biol. Biochem. 35, 225-243, 2003.

Grant, R.F. and Pattey, E.: Temperature sensitivity of N_2O emissions from fertilized agricultural soils: mathematical modelling in *ecosys.* Global Biogeochem. Cycles 22, GB4019, doi:10.1029/2008GB003273, 2008.

Grant, R.F., Pattey, E.M., Goddard, T.W., Kryzanowski, L.M. and Puurveen, H.: Modelling the effects of fertilizer application rate on nitrous oxide emissions from agricultural fields. Soil Sci Soc. Amer. J. 70, 235-248, 2006.

Grant, R.F. Baldocchi, D.D. and Ma, S.: Ecological controls on net ecosystem productivity of a Mediterranean grassland under current and future climates. Agric. For Meteorol. 152: 189– 200, 2012.

Imer, D., Merbold, L., Eugster, W. and Buchmann, N.: Temporal and spatial variations of soil CO_2, CH_4 and N_2O fluxes at three differently managed grasslands. Biogeosci. 10, 5931–5945, 2013.

Jackson, R.D., Oates, L.G., Schacht, W.H., Klopfenstein, T.J., Undersander, D.J., Greenquist, M.A., Bell, M.M. and Gratton, C.: Nitrous oxide emissions from cool-season pastures under managed grazing. Nutr Cycl Agroecosyst 101, 365–376, 2015,

Li, Y., Chen, D., Zhang, Y., Edis, R. and Ding, H.: Comparison of three modeling approaches for simulating denitrification and nitrous oxide emissions from loam-textured arable soils, Global Biogeochem. Cycles 19, GB3002, doi:10.1029/2004GB002392, 2005

Biogeosciences Discuss., doi:10.5194/bg-2015-621, 2016
Manuscript under review for journal Biogeosciences
Published: 18 January 2016

Lu, Y., Huang, Y., Zou, J. and Zheng, X.: An inventory of N_2O emissions from agriculture in China using precipitation-rectified emission factor and background emission, Chemosphere 65, 1915-1924, 2006.

Metivier, K.A., Pattey, E. and Grant, R.F.: Using the ecosys mathematical model to simulate temporal variability of nitrous oxide emissions from a fertilized agricultural soil. Soil Biol. Biochem. 41, 2370–2386, 2009.

Neftel, A., Blatter, A., Schmid, M., Lehmann, B. and Tarakanov, S.V.: An experimental determination of the scale length of N_2O in the soil of a grassland. J. Geophys. Res. 105, 12095–12103, 2000.

Neftel, A, Ammann, C., Fischer, F., Spirig, C., Conen, F., Emmenegger, L , Tuzson, B and Wahlen, S.: N_2O exchange over managed grassland: Application of a quantum cascade laser spectrometer for micrometeorological flux measurements Agric. For. Meteorol. 150, 775–785, 2010.

Pal, P., Clough, T.J., Kelliher, F.M. and. Sherlock, R.R: Nitrous oxide emissions from in situ deposition of 15N-labeled ryegrass litter in a pasture soil. J. Environ. Qual. 42, 323–331, 2013

Pedersen, A.R., Petersen, S.O. and Schelde, K.: A comprehensive approach to soil-atmosphere trace-gas flux estimation with static chambers. European Journal of Soil Science, 61, 888–902, 2010.

Rafique, R., Hennessy, D. and Kiely, G.: Nitrous oxide emission from grazed grassland under different management systems. Ecosystems 14: 563–582, 2011.

Ruzjerez, B.E., White, R.E. and Ball, P.R.: Long-term measurement of denitrification in three contrasting pastures grazed by sheep. Soil Biol Biochem 26:29–39, 1994.

Saxton, K.E., Rawls, W.J., Romberger, J.S. and Papendick, R. I.: Estimating generalized soil-water characteristics from texture. Soil Sci. Soc. Amer. J. 50(4), 1031-1036, 1986.

Schmid, M., Neftel, A., Riedo, M. and Fuhrer, J.:. Process-based modelling of nitrous oxide emissions from different nitrogen sources in mown grassland. Nutr. Cycl. Agroecosyst. 60, 177-187, 2001,

van der Weerden T.J., Clough, T.J. and Styles, T.M.: Using near-continuous measurements of N_2O emission from urine-affected soil to guide manual gas sampling regimes. New Zealand J. Agric. Res. 56, 60-76, 2013.

Biogeosciences Discuss., doi:10.5194/bg-2015-621, 2016
Manuscript under review for journal Biogeosciences
Published: 18 January 2016

Table 1. Key soil properties of the Eutri-Stagnic Cambisol at Oensingen as used in *ecosys*.

Depth	**BD**[¶]	**TOC**	**TON**	**FC**[†]	**WP**[†]	**K_{sat}**[†]	**pH**	**Sand**[‡]	**Silt**[‡]	**Clay**[‡]	**CF**
m	Mg m^{-3}	g kg^{-1}	g kg^{-1}	m^3 m^{-3}	m^3 m^{-3}	mm h^{-1}		g kg^{-1}	g kg^{-1}	g kg^{-1}	m^3 m^{-3}
0.01	1.21	27.2	2900	0.382	0.223	3.4	7	240	330	430	0
0.03	1.21	27.2	2900	0.382	0.223	3.4	7	240	330	430	0
0.07	1.21	27.2	2900	0.382	0.223	3.4	7	240	330	430	0
0.13	1.24	27.2	2900	0.391	0.234	3.4	7	240	330	430	0
0.28	1.28	20.2	2100	0.403	0.24	2.4	7	180	380	440	0
0.6	1.28	11.6	1100	0.403	0.24	1.4	7	180	380	440	0
0.7	1.28	11.6	1100	0.403	0.24	1.4	7	180	380	440	0
0.9	1.28	9	900	0.403	0.24	1.4	7	180	380	440	0
1.5	1.28	6	600	0.403	0.24	1.4	7	180	380	440	0.1

[¶] abbreviations BD: bulk density, TOC and TON: total organic C and N, FC: field capacity, WP: wilting point, K_{sat}: saturated hydraulic conductivity, CF: coarse fragments.

[†] Values from pedotransfer functions in Saxton et al. (1986).

[‡] Sand, silt and clay contents were recalculated in *ecosys* to account for SOC and coarse fragments if any.

Table 2. Plant and soil management operations at the Oensingen intensively managed grassland from 2004 to 2009.

Year	Plant Management		Soil Management					
	Date	Management	Date	Management	Amount (g m^{-2})			
					NH_4^+	NO_3^-	ON	OC
2001			07 May	tillage				
			10 May	tillage				
	11 May	planting	15 June	mineral fertilizer	1.5	1.5		
	1 July	harvest	12 July	mineral fertilizer	1.5	1.5		
	8 Aug.	harvest	16 Aug.	mineral fertilizer	1.15	1.15		
	12 Sep.	harvest						
	31 Oct.	harvest						
2002			12 Mar.	mineral fertilizer	1.5	1.5		
	15 May	harvest	22 May	manure slurry	4.2		2.8	31.2
	25 June	harvest	1 July	mineral fertilizer	1.75	1.75		
	15 Aug.	harvest	18 Aug.	manure slurry	5.9		5.3	49.6
	18 Sep.	harvest	30 Sep.	mineral fertilizer	1.5	1.5		
	07 Dec.	harvest						
2003			18 Mar.	manure slurry	5.9		5.3	61.1
	30 May	harvest	02 June	mineral fertilizer	1.5	1.5		
	04 Aug.	harvest	18 Aug.	manure slurry	6.3		1.9	19.0
	13 Oct.	harvest						
2004			17 Mar.	manure slurry	5.0		1.5	19.5
	11 May	harvest	17 May	mineral fertilizer	1.5	1.5		
	25 June	harvest	01 July	manure slurry	5.5		0.5	9.9
	28 Aug.	harvest	31 Aug.	mineral fertilizer	1.5	1.5		
	03 Nov.	harvest						
2005			29 Mar.	manure slurry	6.7		3.1	42.0
	10 May	harvest	17 May	mineral fertilizer	1.5	1.5		
	27 June	harvest	05 July	manure slurry	5.0		3.5	59.6
	29 Aug.	harvest	16 Sep.	mineral fertilizer	1.5	1.5		
	24 Oct.	harvest						
2006	24 May	harvest						
	05 July	harvest	13 July	manure slurry	4.7		1.4	12.5
	12 Sep.	harvest	27 Sep.	manure slurry	4.4		1.3	13.6

Biogeosciences Discuss., doi:10.5194/bg-2015-621, 2016
Manuscript under review for journal Biogeosciences
Published: 18 January 2016

	26 Oct.	harvest	30 Oct.	manure slurry	6.4		3.2	57.8
2007			03 Apr.	manure slurry	5.2		4.6	75.1
	26 Apr.	harvest	03 May	mineral fertilizer	1.5	1.5		
	06 July	harvest	13 July	manure slurry	4.9		1.8	45.9
	23 Aug.	harvest	28 Aug.	mineral fertilizer	1.5	1.5		
	11 Oct.	harvest	24 Oct.	manure slurry	4.6		3.0	38.9
	19 Dec.	terminate	19 Dec.	plowing				
2008			01 May	tillage				
			04 May	tillage				
	05 May	planting						
	01 July	harvest	10 July	mineral fertilizer	1.5	1.5		
	29 July	harvest	07 Aug.	mineral fertilizer	1.5	1.5		
	08 Sep.	harvest	19 Sep.	manure slurry	2.9		0.5	8.6
	07 Nov.	harvest						
2009			07 Apr.	mineral fertilizer	1.5	1.5		
	01 May	harvest	12 May	manure slurry	4.4		1.6	26.0
	16 June	harvest	06 Aug.	manure slurry	3.3		1.2	19.0
	29 July	harvest						
	07 Sep.	harvest	15 Sep.	mineral fertilizer	6.5(urea)			
	20 Oct.	harvest						

Biogeosciences Discuss., doi:10.5194/bg-2015-621, 2016
Manuscript under review for journal Biogeosciences
Published: 18 January 2016

Table 3. Gross primary productivity (GPP), ecosystem respiration (R_e), net ecosystem productivity (NEP), harvest, net biome productivity (NBP) and N_2O emissions derived from EC or chambers and modelled (M) with current defoliation practices (current), with defoliation increased so that LAI remaining after defoliation was reduced by one-half (increase), and with defoliation increased and delayed by 5 days (+ delay). Positive values indicate uptake, negative values emissions.

Year		2002	2003	2004	2005	2006	2007	2008	2009
Precip.(mm)		1478	817	1158	966	1566	1328	1188	1004
MAT (°C)		9.56	9.58	8.92	8.67	9.30	9.59	9.30	9.48
GPP	EC	2159	1773	2058	1766	1817	2102	1455	2119
(g C m^{-2} y^{-1})	M: current	2214	1836	2220	2111	1953	2539	1419	1852
	: increase	2064	1764	2054	1969	1865	2285	1305	1705
	: + del ay	2014	1774	2076	1966	1771	2277	1225	1686
R_e	EC	-1490	-1558	-1541	-1565	-1577	-1684	-1450	-1657
(g C m^{-2} y^{-1})	M: current	-1560	-1421	-1704	-1679	-1680	-1935	-1366	-1373
	: increase	-1457	-1345	-1569	-1572	-1579	-1714	-1212	-1259
	: + del ay	-1458	-1350	-1541	-1517	-1519	-1679	-1183	-1235
NEP	EC	669	215	517	201	240	418	5	462
(g C m^{-2} y^{-1})	M: current	654	415	516	432	273	604	53	479
	: increase	607	419	485	397	286	571	93	446
	: + del ay	556	414	535	449	252	598	42	451
Harvest	field	462	241	401	247	232	448	293	532
(g C m^{-2} y^{-1})	M: current	570	314	525	460	421	690	308	487
	: increase	561	360	465	497	455	678	314	484
	: + del ay	537	353	579	513	446	686	262	473
C inputs		81	80	29	102	84	160	9	45
NBP	field	288	54	145	56	92	130	-279	-25
(g C m^{-2} y^{-1})	M: current	165	181	20	74	-64	74	-246	37
	: increase	127	139	49	2	-85	53	-212	7
	: + del ay	101	141	-15	38	-110	72	-211	23
N inputs		27.6	22.5	18.5	24.3	21.4	30.1	9.4	20.0
N_2O	chamber	-0.130	-0.050	-0.060	-0.230	-0.020	-0.280	-0.480	-0.510
(g N m^{-2} y^{-1})	(range)	-0.450	-0.180	-0.180	-0.320	-0.060	-0.350	-0.620	-0.680
	M: current	-0.302	-0.209	-0.183	-0.193	-0.220	-0.281	-0.326	-0.366
	: increase	-0.269	-0.215	-0.250	-0.249	-0.318	-0.312	-0.335	-0.318
	: + del ay	-0.284	-0.234	-0.347	-0.352	-0.273	-0.348	-0.327	-0.395

Biogeosciences Discuss., doi:10.5194/bg-2015-621, 2016
Manuscript under review for journal Biogeosciences
Published: 18 January 2016

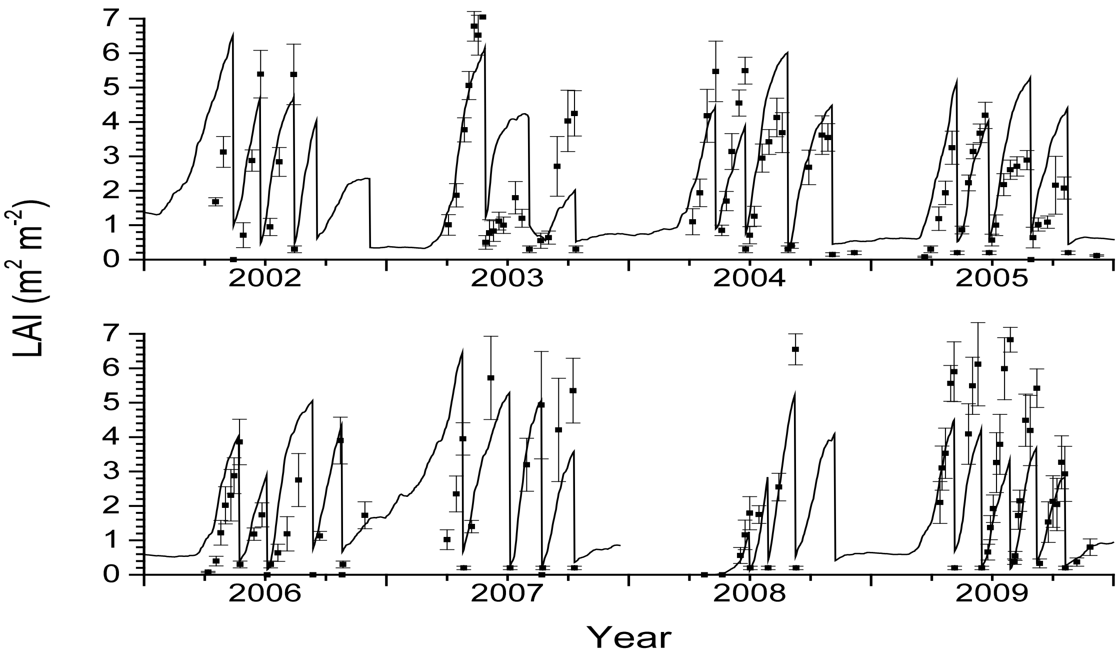

Fig. 1. LAI measured (symbols) and modelled (lines) from 2002 through 2009 at the Oensingen intensively managed grassland.

Biogeosciences Discuss., doi:10.5194/bg-2015-621, 2016
Manuscript under review for journal Biogeosciences
Published: 18 January 2016

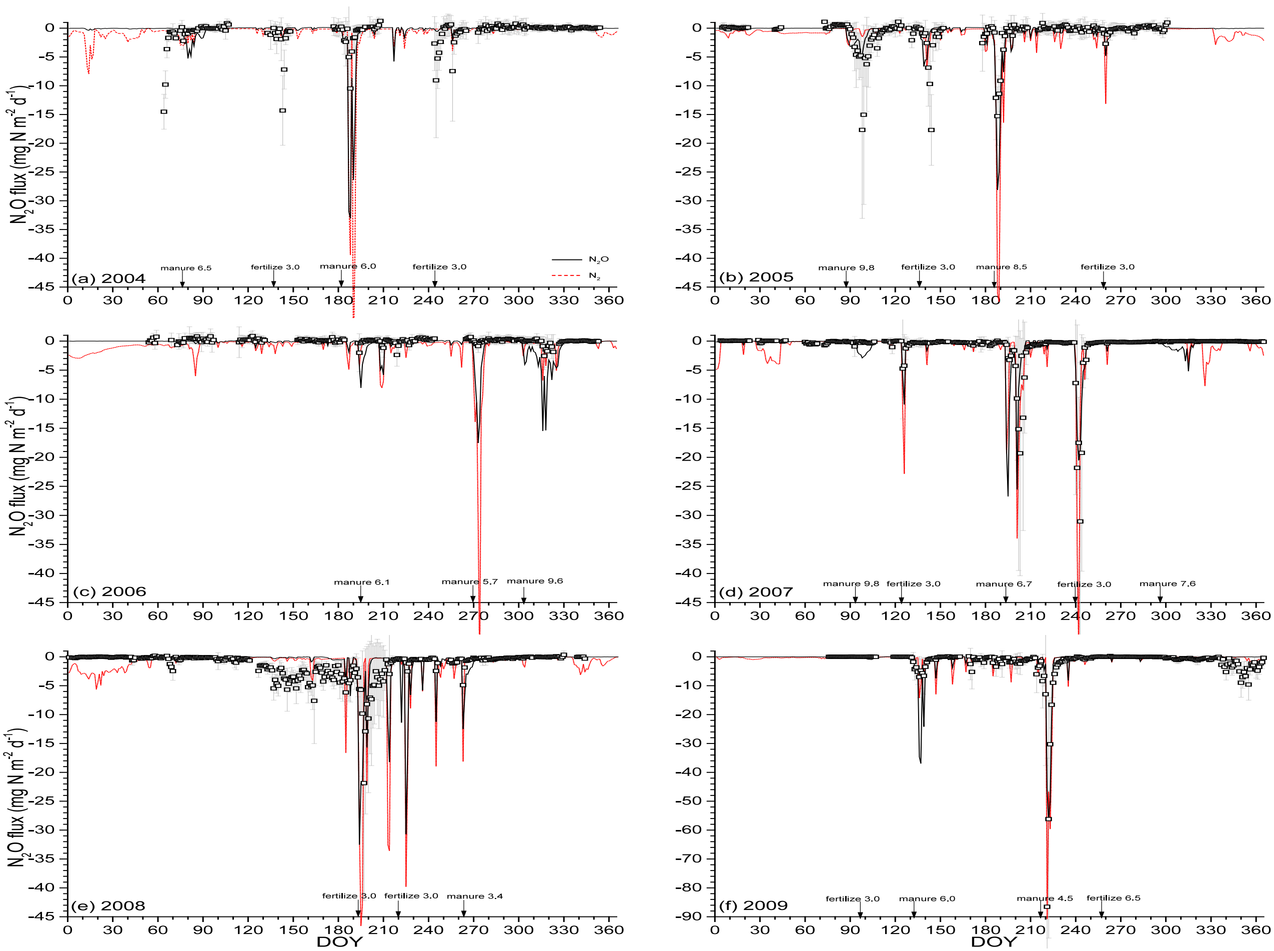

Fig. 2. Daily-aggregated N_2O emissions measured (symbols) and N_2O and N_2 emissions modelled (lines) from 2004 through 2009 at the Oensingen intensively managed grassland. Numbers with each fertilizer or manure addition indicate total N (g N m^{-2}). Negative values indicate effluxes to the atmosphere.

Biogeosciences Discuss., doi:10.5194/bg-2015-621, 2016
Manuscript under review for journal Biogeosciences
Published: 18 January 2016

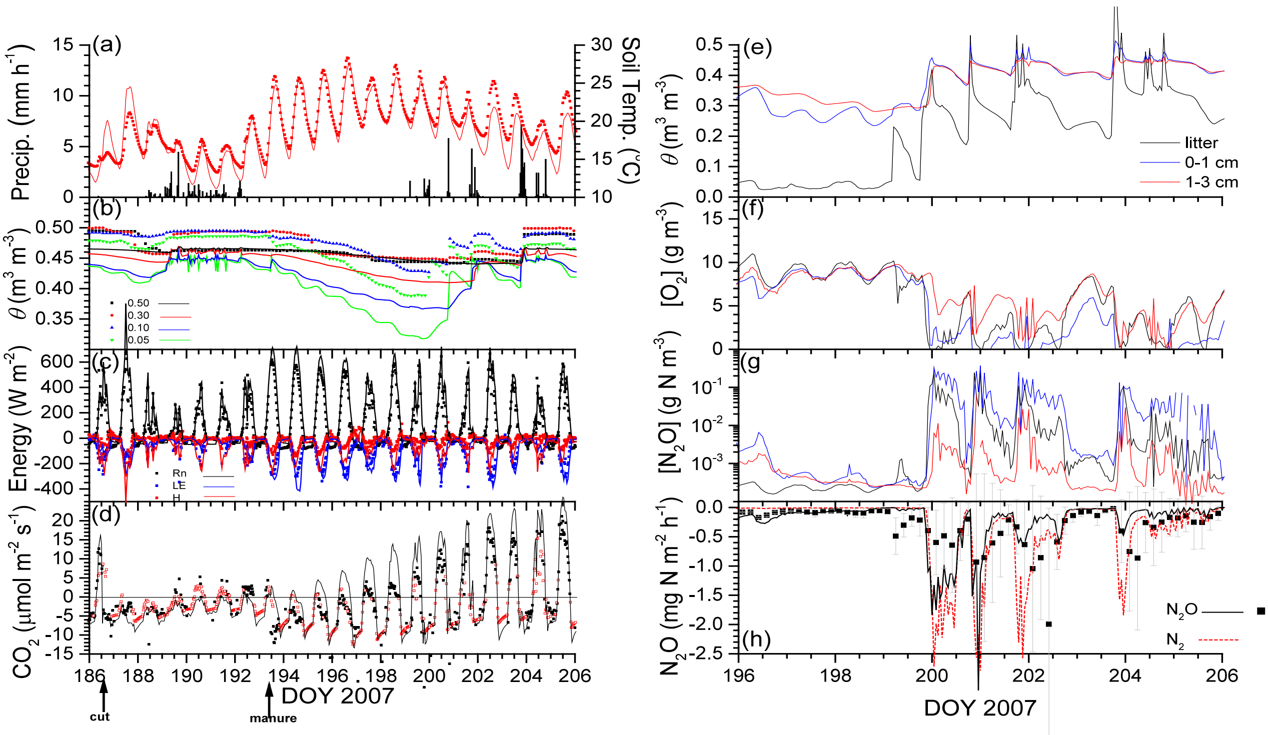

Fig. 3. (a) Precipitation and soil temperature at 0.05 m, (b) soil water content (θ) at 0.05, 0.10, 0.30 and 0.50 m, (c) energy and (d) CO_2 fluxes measured (closed symbols), gap-filled (open symbols) and modelled (lines) during 20 days from harvest (cut) to then end of the emission event following manure application (manure) in July 2007. (e) θ, (f and g) aqueous concentrations of O_2 and N_2O modelled in the surface litter and at 0.01 and 0.02 m in the soil, and (h) N_2O and N_2 fluxes measured (symbols) and modelled (lines) during the last 10 days of this period when the emission event occurred. For fluxes, positive values represent influxes to the soil, negative values effluxes to the atmosphere.

Biogeosciences Discuss., doi:10.5194/bg-2015-621, 2016
Manuscript under review for journal Biogeosciences
Published: 18 January 2016

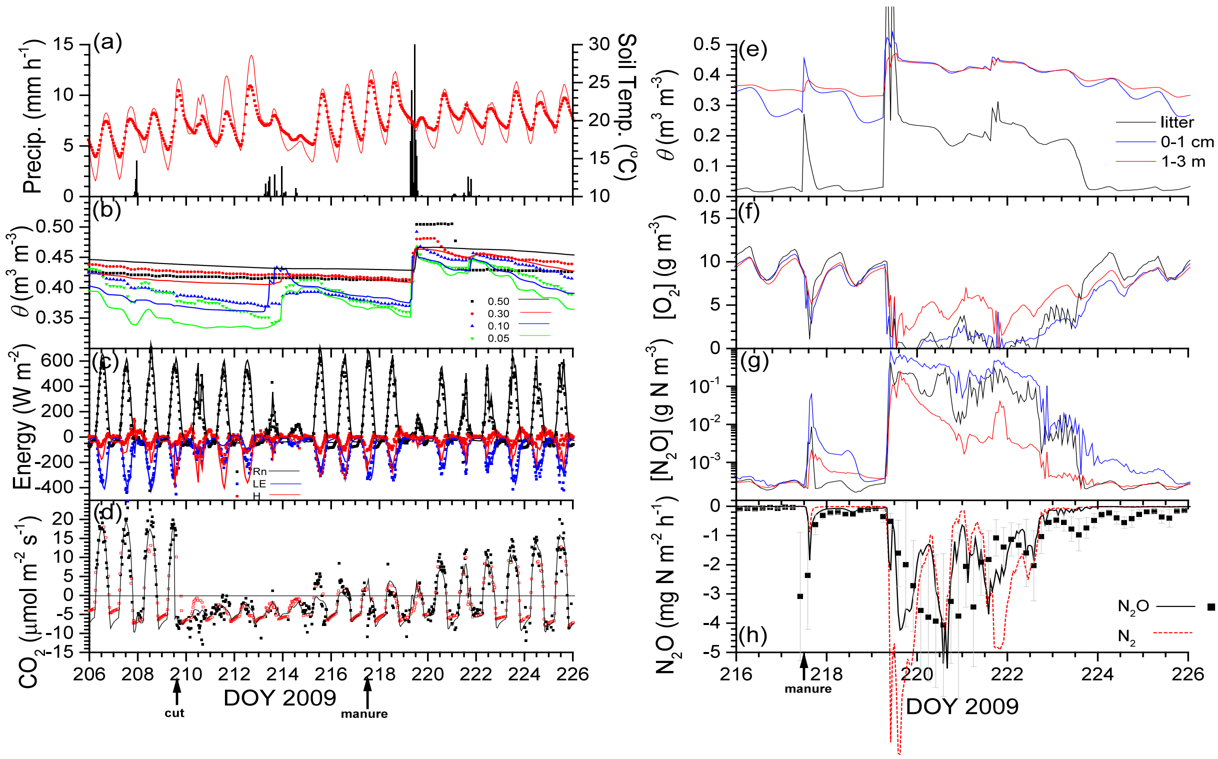

Fig. 4. (a) Precipitation and soil temperature at 0.05 m, (b) soil water content (θ) at 0.05, 0.10, 0.30 and 0.50 m, (c) energy and (d) CO_2 fluxes measured (closed symbols), gap-filled (open symbols) and modelled (lines) during 20 days from harvest (cut) to then end of the emission event following manure application (manure) in August 2008. (e) θ, (f and g) aqueous concentrations of O_2 and N_2O modelled in the surface litter and at 0.01 and 0.02 m in the soil, and (h) N_2O and N_2 fluxes measured (symbols) and modelled (lines) during the last 10 days of this period when the emission event occurred. For fluxes, positive values represent influxes to the soil, negative values effluxes to the atmosphere.

Biogeosciences Discuss., doi:10.5194/bg-2015-621, 2016
Manuscript under review for journal Biogeosciences
Published: 18 January 2016

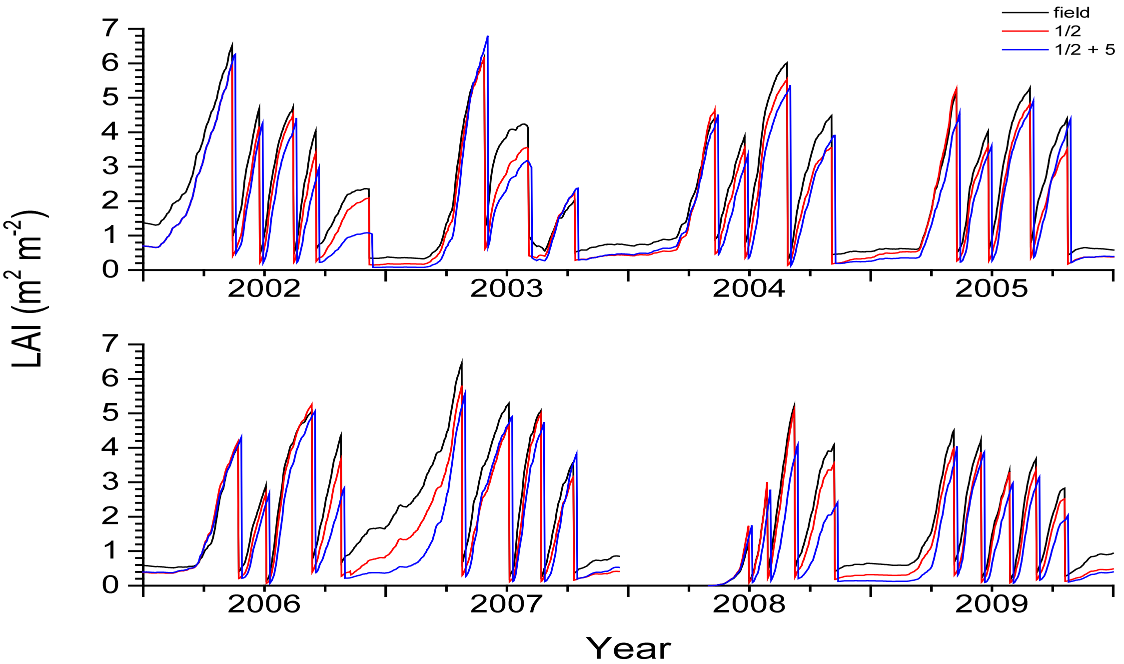

Fig. 5. LAI modelled from 2002 through 2009, with LAI after each cut reduced to one-half of that estimated from the field experiment without or with a delay of 5 days at the Oensingen intensively managed grassland.

Biogeosciences Discuss., doi:10.5194/bg-2015-621, 2016
Manuscript under review for journal Biogeosciences
Published: 18 January 2016

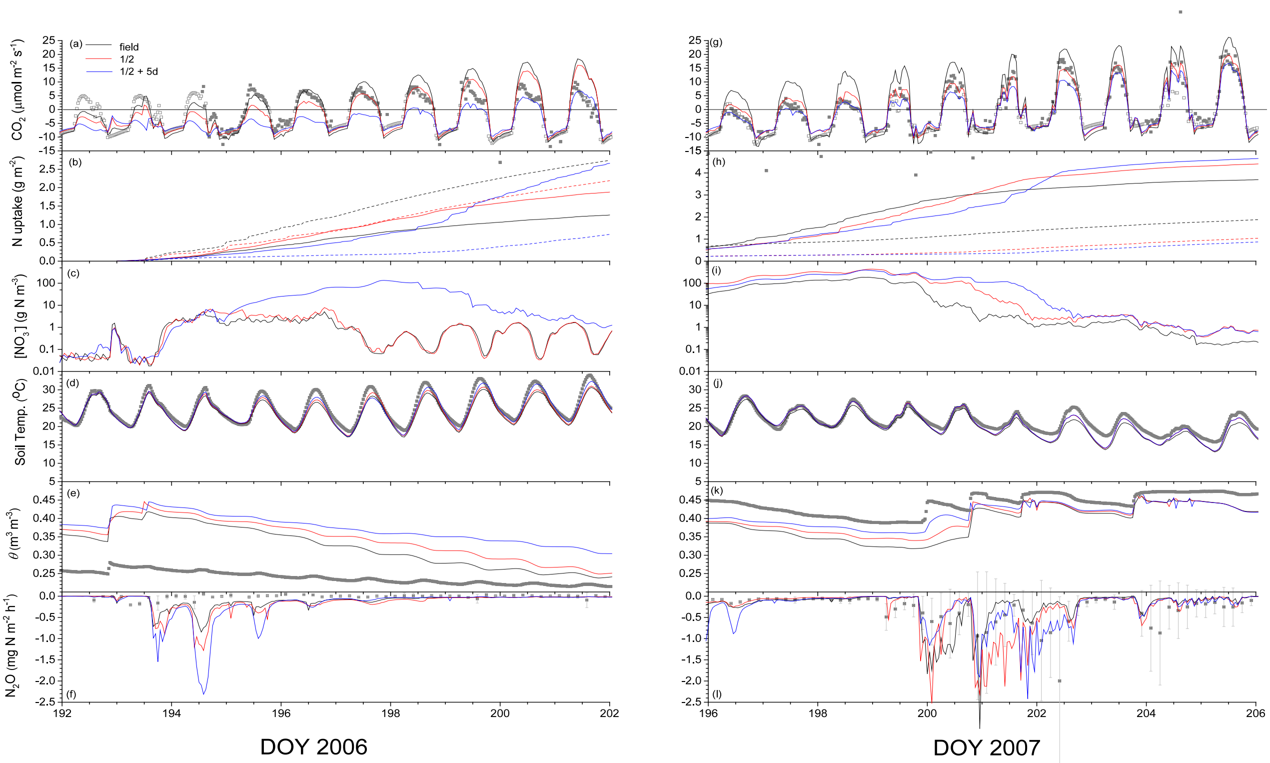

Fig. 6. (a,g) CO_2 fluxes, (b,h) cumulative NH_4^+ (dashed) and NO_3^- (solid) uptake since manure application, (c,i) aqueous NO_3^- concentrations at 0 – 1 cm, (d,j) T_s and (e,k) θ at 5 cm, and (f,l) N_2O fluxes measured (symbols) and modelled (lines) with LAI after each cut reduced to one-half of that estimated from the field experiment without or with a delay of 5 days during emission events following manure applications on DOY 194 in (a-f) 2006 and (g-l) 2007 (see Table 2). For fluxes, positive values represent influxes to the soil, negative values effluxes to the atmosphere.

Biogeosciences Discuss., doi:10.5194/bg-2015-621, 2016
Manuscript under review for journal Biogeosciences
Published: 18 January 2016

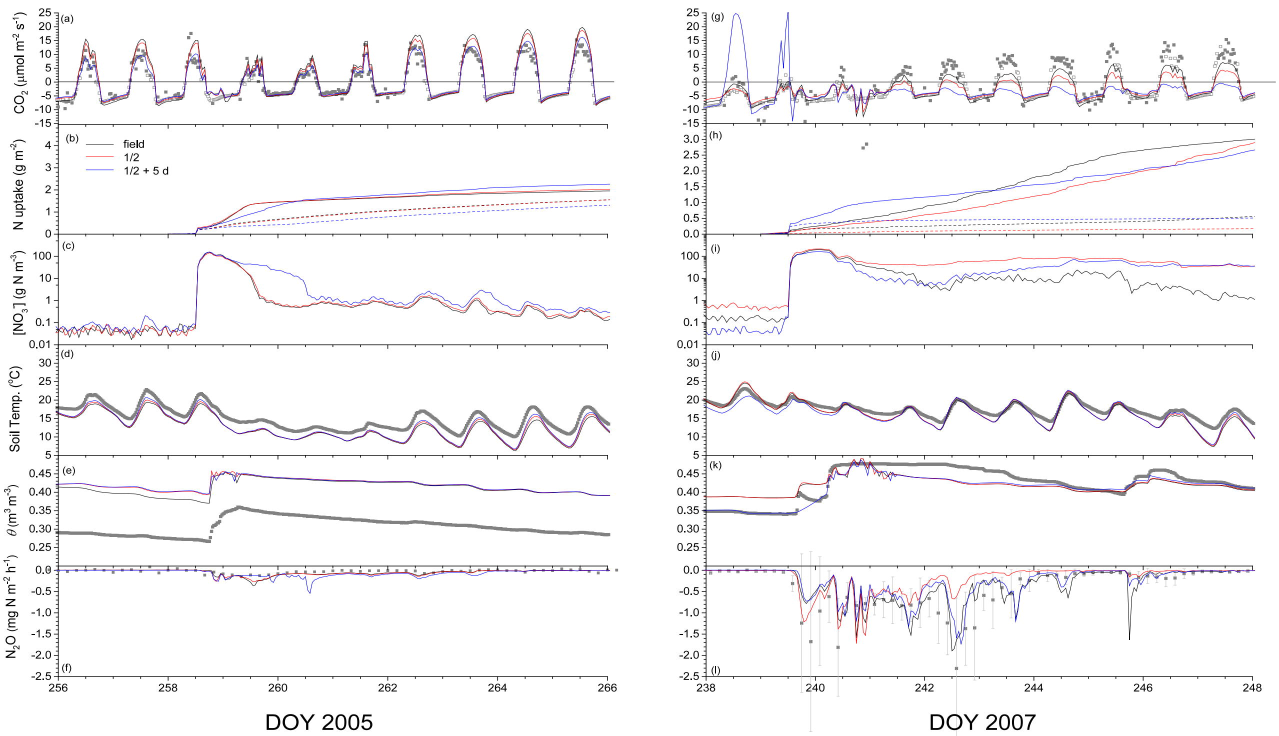

Fig. 7 (a,g) CO_2 fluxes, (b,h) cumulative NH_4^+ (dashed) and NO_3^- (solid) uptake since manure application, (c,i) aqueous NO_3^- concentrations at 0 – 1 cm, (d,j) T_s and (e,k) θ at 5 cm, and (f,l) N_2O fluxes measured (symbols) and modelled (lines) with LAI after each cut reduced to one-half of that estimated from the field experiment without or with a delay of 5 days during emission events following fertilizer applications on DOY 259 in 2005 (a-f) and DOY 240 in 2007 (g-l) (see Table 2). For fluxes, positive values represent influxes to the soil, negative values effluxes to the atmosphere.